

## Sensing the Chirality of Dawson Lanthanide Polyoxometalates $[\alpha_1\text{-LnP}_2\text{W}_{17}\text{O}_{61}]^{7-}$ by Multinuclear NMR Spectroscopy

Cécile Boglio,<sup>[a, b]</sup> Bernold Hasenknopf,<sup>[a]</sup> Géraldine Lenoble,<sup>[a]</sup> Pauline Rémy,<sup>[a, b]</sup> Pierre Gouzerh,<sup>[a]</sup> Serge Thorimbert,<sup>[b]</sup> Emmanuel Lacôte,<sup>[b]</sup> Max Malacria,<sup>\*, [b]</sup> and René Thouvenot<sup>\*, [a]</sup>

**Abstract:** Lanthanide complexes of the chiral Dawson phosphotungstate  $[\alpha_1\text{-P}_2\text{W}_{17}\text{O}_{61}]^{10-}$  were used to study the formation of diastereomers with optically pure organic ligands. The present work started with the full assignment of the  $^{183}\text{W}$  NMR spectra of  $[\alpha_1\text{-Yb}(\text{H}_2\text{O})_4\text{P}_2\text{W}_{17}\text{O}_{61}]^{7-}$  at different temperatures and concentrations, which allowed the structure of the dimerized form in aqueous solution to be established. Different enantiopure amino acids and phosphonic acids were

screened as ligands. Both types allowed chiral differentiation by multinuclear NMR spectroscopy under fast-exchange conditions. Functional groups with a good affinity for the oxo framework of the polyoxometalate were identified, and maps of the interactions between L-serine and *N*-phosphono-

methyl-L-proline with  $[\alpha_1\text{-Yb}(\text{H}_2\text{O})_4\text{P}_2\text{W}_{17}\text{O}_{61}]^{7-}$  were established. This demonstrates the power of  $^{183}\text{W}$  NMR spectroscopy to elucidate the molecular recognition of inorganic molecules by organic compounds. *N*-Phosphonomethyl-L-proline appears to be a convenient ligand to promote separation of the diastereomers and ultimately resolution of the enantiomers of  $[\alpha_1\text{-Yb}(\text{H}_2\text{O})_4\text{P}_2\text{W}_{17}\text{O}_{61}]^{7-}$ .

**Keywords:** chirality • lanthanides • NMR spectroscopy • polyoxometalates • tungsten

### Introduction

Polyoxometalates (POMs) are early transition metal oxo clusters with diverse compositions, structures, and properties that result in a variety of applications in organic synthesis,

materials science, and biology.<sup>[1–3]</sup> Each of these fields would benefit from readier availability of optically active polyoxometalates, but their preparation remains a challenge. Several strategies have been applied to solve this problem. First, polyoxometalates can be rendered chiral by attachment of chiral organic ligands.<sup>[4–10]</sup> Analogously, POM-based solid-state architectures can be rendered chiral by this approach.<sup>[11–13]</sup> In these cases, however, the polyoxometalate framework remains essentially achiral. Hill et al. have shown that it is possible to transfer the chirality of specific organic molecules to build enantiomerically pure polyoxometalates with a chiral framework.<sup>[14]</sup> Yet, the organic component remains covalently bound to the inorganic cluster. A number of chiral polyoxometalates reported in the literature have all been prepared as racemic mixtures.<sup>[15–20]</sup> To the best of our knowledge, resolution of  $[\text{H}_4\text{Co}_2\text{Mo}_{10}\text{O}_{38}]^{6-}$  with optically pure  $[\text{Co}(\text{en})_3]^{3+}$  by Ama et al. is the only example of preparative separation of two enantiomers in polyoxometalate chemistry.<sup>[21–23]</sup> Partial spontaneous resolution<sup>[24]</sup> and more recently full spontaneous resolution<sup>[25,26]</sup> have been observed. These sparse reports certainly reflect the little available knowledge on molecular recognition of polyoxometalates. Indeed, a suitable resolving agent for polyoxometalates must recognize a chiral oxide surface. Observations of

[a] Dr. C. Boglio, Dr. B. Hasenknopf, Dr. G. Lenoble, Dr. P. Rémy, Prof. Dr. P. Gouzerh, Dr. R. Thouvenot  
Laboratoire de chimie inorganique et matériaux moléculaires (UMR CNRS 7071)  
Institut de chimie moléculaire (FR 2769)  
Université Pierre et Marie Curie-Paris 6  
Case courrier 42, 4 place Jussieu, 75252 Paris cedex 05 (France)  
Fax: (+33)144-273-841  
E-mail: rth@ccr.jussieu.fr

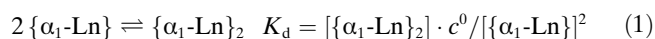
[b] Dr. C. Boglio, Dr. P. Rémy, Dr. S. Thorimbert, Dr. E. Lacôte, Prof. Dr. M. Malacria  
Laboratoire de chimie organique (UMR CNRS 7611)  
Institut de chimie moléculaire (FR 2769)  
Université Pierre et Marie Curie-Paris 6  
Case courrier 229, 4 place Jussieu, 75252 Paris cedex 05 (France)  
Fax: (+33)144-277-360  
E-mail: malacria@ccr.jussieu.fr

Supporting information for this article is available on the WWW under <http://www.chemeurj.org/> or from the author.

a Pfeiffer effect<sup>[27]</sup> or an induced Cotton effect indicate enantioselective interactions of polyoxometalates with chiral ammonium ions or sugar molecules.<sup>[28–31]</sup> One such system was used for asymmetric polymerization of benzyl alcohol.<sup>[32]</sup> Stereoelectronic interactions with amino acids were also observed by NMR spectroscopy.<sup>[16,18]</sup> In particular, Sadakane et al. have differentiated the two enantiomers of  $[\alpha_1\text{-Ce}(\text{H}_2\text{O})_x\text{P}_2\text{W}_{17}\text{O}_{61}]^{7-}$  ( $\{\alpha_1\text{-Ce}\}$ ) by complexation with optically active amino acids.<sup>[33]</sup> This work is of interest, because we have shown recently that analogous complexes in this family  $[\alpha_1\text{-Ln}^{\text{III}}(\text{H}_2\text{O})_4\text{P}_2\text{W}_{17}\text{O}_{61}]^{7-}$  ( $\{\alpha_1\text{-Ln}\}$ ; Ln = La, Sm, Eu, Yb) are active Lewis acid catalysts in organic transformations.<sup>[34,35]</sup> Studying the interactions of these compounds with asymmetric molecules is therefore a prerequisite to understand the role of the polyoxometalate in stereoselective reactions. We therefore used <sup>183</sup>W and <sup>31</sup>P NMR spectroscopy to map the interactions between organic ligands and  $\{\alpha_1\text{-Yb}\}$  to design a method of optical resolution and enantioselective catalysis.

## Methodology

Peacock–Weakley-type complexes of lanthanides with the  $\alpha_1$  isomer of the monolacunary Dawson polyoxometalate  $[\text{P}_2\text{W}_{17}\text{O}_{61}]^{10-}$  are well described in the literature.<sup>[33,36–44]</sup> Their coordination chemistry is similar to that of the achiral  $\alpha_2$  isomer.<sup>[37,41,45–52]</sup> Multiple diastereomers are formed when one lanthanide ion is sandwiched between two  $\alpha_1\text{-}[\text{P}_2\text{W}_{17}\text{O}_{61}]^{10-}$  ions to yield  $[\text{Ln}(\alpha_1\text{-P}_2\text{W}_{17}\text{O}_{61})_2]^{17-}$ ,<sup>[53]</sup> comparable to the situation with the chiral Keggin derivative  $[\text{Ln}(\beta_2\text{-SiW}_{11}\text{O}_{39})_2]$ .<sup>[54]</sup> We focus here on  $\{\alpha_1\text{-Ln}\}$ , that is, 1:1 Ln:POM complexes, which occur as two enantiomers. They are in equilibrium with the dimer in aqueous solution according to Equation (1).



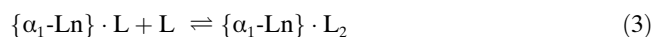
The dimer is formed by coordination of a terminal oxo ligand of each monomer complex to the lanthanide ion of the other monomer. Two dimeric structures have been identified in the solid state, which differ in the site of the W–O–Ln bridge. In  $\{\alpha_1\text{-La}\}_2$ , capping W=O groups form the bridge,<sup>[44]</sup> while in  $\{\alpha_1\text{-Ce}\}_2$  belt W=O groups are involved.<sup>[33]</sup>

These polyoxometalates contain two nonequivalent phosphorus atoms: P1 in the  $\{\text{LnPW}_8\text{O}_{34}\}$  moiety, and P2 in the  $\{\text{PW}_9\text{O}_{34}\}$  moiety. According to <sup>31</sup>P NMR spectroscopy, which gives only two resonance signals whatever the concentration, one for P1 and one for P2, the monomer–dimer equilibrium is in the fast-exchange regime at room temperature on the <sup>31</sup>P NMR timescale. From the concentration dependence of the observed chemical shifts, Pope et al. calculated the dimerization constant of  $\{\alpha_1\text{-Ce}\}$  to be  $K_d = 20 \pm 4$  at 22 °C.<sup>[33]</sup> Using the same approach, we found  $K_d = 23 \pm 6$  at 25 °C for  $\{\alpha_1\text{-Yb}\}$ . This means that at a typical concentration of 200 mg mL<sup>-1</sup> for our <sup>31</sup>P NMR spectra, about 50 % of the complex is in the form of the dimer.

On addition of an organic ligand L that can coordinate to the lanthanide ion, new complexes are formed with the monomer.<sup>[55]</sup> For steric reasons, coordination to the lanthanide centers in the dimer can be excluded for L of the size of amino acids.<sup>[33,56]</sup> We consider here the coordination of one L to yield  $[\alpha_1\text{-LnL}(\text{H}_2\text{O})_x\text{P}_2\text{W}_{17}\text{O}_{61}]^{7-}$   $[\alpha_1\text{-Ln}] \cdot \text{L}$ , Eq. (2), and that of two L to yield  $[\alpha_1\text{-LnL}_2(\text{H}_2\text{O})_y\text{P}_2\text{W}_{17}\text{O}_{61}]^{7-}$   $[\alpha_1\text{-Ln}] \cdot \text{L}_2$ , Eq. (3).



$$K_{11} = \frac{[\{\alpha_1\text{-Ln}\} \cdot \text{L}] \cdot c^0}{([\{\alpha_1\text{-Ln}\}] \cdot [\text{L}])}$$



$$K_{12} = \frac{[\{\alpha_1\text{-Ln}\} \cdot \text{L}_2] \cdot c^0}{([\{\alpha_1\text{-Ln}\} \cdot \text{L}] \cdot [\text{L}])}$$

Under fast-equilibrium conditions, the observed NMR signal for each nucleus is the mean value of the chemical shifts of the monomer ( $\delta_M$ ), the dimer ( $\delta_D$ ), and the complexes with L ( $\delta_{M \cdot L}$ ,  $\delta_{M \cdot L_2}$ ). A full analysis of the species present in solution cannot be achieved with a single NMR experiment, and only recording of spectra at different concentrations gives insight into the distribution of species.

With regard to the interactions of  $\{\alpha_1\text{-Ln}\}$  with chiral ligands under conditions of fast ligand exchange, the splitting of the NMR signals provides important information. Indeed, the reaction of racemic  $\{(\pm)\text{-}\alpha_1\text{-Ln}\}$  with an enantiopure ligand L\* yields two diastereomers  $\{(+)\text{-}\alpha_1\text{-Ln}\} \cdot \text{L}^*$  and  $\{(-)\text{-}\alpha_1\text{-Ln}\} \cdot \text{L}^*$  [considering only Eq. (2)]. The presence of both isomers in solution can be detected by NMR spectroscopy, as long as the racemization of  $\{\alpha_1\text{-Ln}\}$  is slow on the NMR timescale. Two signals ( $\delta_{\text{obs}A}$  and  $\delta_{\text{obs}B}$ ) should then arise for each nucleus (Figure 1).

The chemical shifts depend on  $\delta_{\text{obs initial}}$  of the unbound  $\{\alpha_1\text{-Ln}\}$  in monomer–dimer equilibrium, on  $\delta_{M \cdot L}$  of the pure diastereomers A and B, and on the formation constants ( $K_{11}A$  and  $(K_{11})B$ ) of the complexes, which determine the

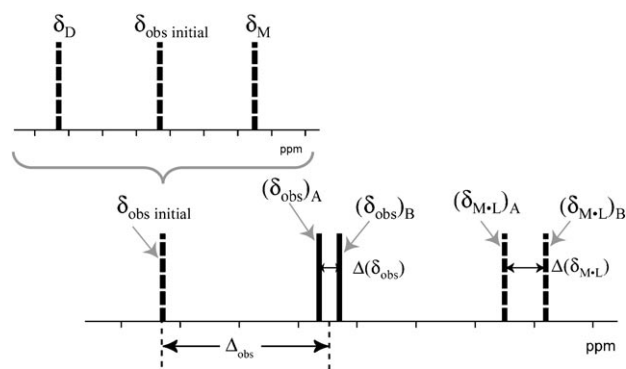


Figure 1. Schematic representation of the differentiation by NMR of a racemic polyoxometalate in monomer–dimer equilibrium on addition of a chiral, optically active ligand L\* in the fast-exchange regime with  $(K_{11})A \approx (K_{11})B$ . M = monomer  $\{\alpha_1\text{-Ln}\}$ ; D = dimer  $\{\alpha_1\text{-Ln}\}_2$ ; A, B = two different diastereomers  $\{\alpha_1\text{-Ln}\} \cdot \text{L}^*$ ; solid lines: observed signals, dotted lines: hypothetical signals for the pure species.

molar fraction of each diastereomer. A large differentiation of the signals  $\Delta(\delta_{\text{obs}})$  can therefore result from a pronounced difference in the complexation constants  $K_{11}$  for the two diastereomers, or from a significantly different chemical environment of the observed nucleus in the two diastereomers, that is, increased  $\Delta(\delta_{\text{M-L}})$ . Actually, the two effects are likely to occur simultaneously, because a larger formation constant should result from tighter binding, so that the chemical environment of the observed nucleus is more strongly affected in that diastereomer. Bearing in mind our objective to find an efficient resolving agent, it then seems reasonable to look for a ligand that causes a large differentiation  $\Delta(\delta_{\text{obs}})$  of the signals. The preparative separation of the two diastereomers would be facilitated if they were present in different concentrations, and if their properties (reflected by their chemical shifts) were highly different.

Note that under these conditions of fast coordination equilibrium, differentiation of a given signal of the racemic  $\{\alpha_1\text{-Ln}\}$  by a chiral ligand will always yield two signals of equal intensity, whatever the respective equilibrium concentrations of the two diastereomers. Diastereomeric excess can only be detected if the chemical shifts  $(\delta_{\text{M-L}})_A$  and  $(\delta_{\text{M-L}})_B$  of the pure diastereomers are known. Furthermore, only one signal will be observed when racemic  $L^*$  is used.

Since the NMR frequency of the  $^{183}\text{W}$  nucleus is lower than that of  $^{31}\text{P}$ , the fast-exchange conditions  $k_{\text{ex}} \gg \Delta\nu$  in  $^{31}\text{P}$  NMR spectroscopy are generally sufficient for fast exchange in  $^{183}\text{W}$  spectra, too. All of the above considerations therefore apply.

## Results and Discussion

**Assignment of  $^{183}\text{W}$  NMR spectra:** We recently published the assignment of all 17 signals of  $\{\alpha_1\text{-Yb}\}$  at very high concentration.<sup>[57]</sup> For solubility reasons, it is not possible to perform complexation studies with organic ligands under these conditions. As  $^{183}\text{W}$  NMR chemical shifts are medium-dependent (concentration, temperature, etc.), it was necessary to record the spectra of  $\{\alpha_1\text{-Yb}\}$  at different dilutions, and to follow the variation of  $\delta$  with the POM concentration (Figure 2 and Supporting Information). Assignment of peaks (numbering of W atoms shown in Figure 3) was made under the assumption of a smooth evolution of the chemical shifts. In addition, the  $^2J_{\text{WW}}$  coupling constants of W5 and W10 at  $c=0.44 \text{ mol L}^{-1}$  were measured, and the variation of  $\delta$  as a function of temperature was used to confirm the assignment. W9 and W10 have negative temperature coefficients in  $\{\alpha_1\text{-Yb}\}$ , and this behavior allows their identification. A spectrum obtained at a given concentration is then assigned by extrapolation from the plots in Figure 2 and Figure S1 in the Supporting Information. It can be seen from these figures that few signals vary significantly with concentration. The largest variation is observed for W5 ( $\Delta\delta > 20 \text{ ppm}$  between  $0.1$  and  $0.5 \text{ mol L}^{-1}$ ), and to a lesser extent for W1 and W10 ( $\Delta\delta < 10 \text{ ppm}$ ), all close to Yb (Figure 3). These variations are attributed to the change in chemical en-

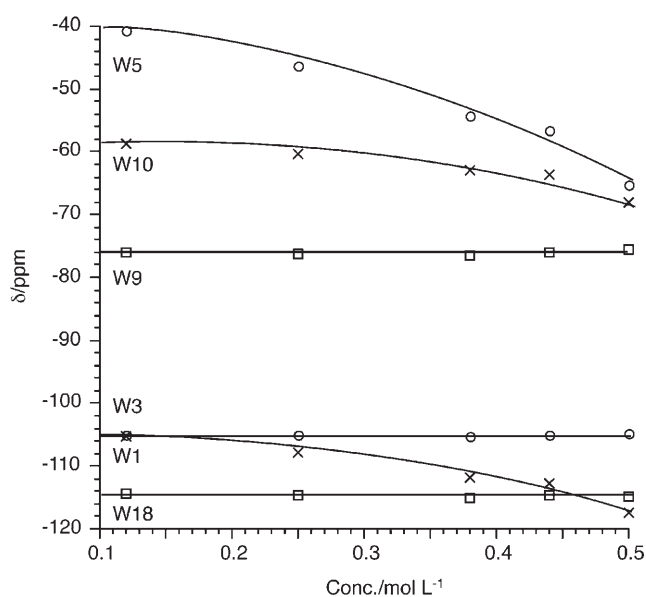


Figure 2.  $^{183}\text{W}$  chemical shifts ( $-40$  to  $-120 \text{ ppm}$  range) of  $[\alpha_1\text{-Yb}(\text{H}_2\text{O})_4\text{P}_2\text{W}_{17}\text{O}_{61}]^{7-}$  as a function of concentration.  $T=300 \text{ K}$ . (see Figure S1 in the Supporting Information for full chemical shift range)

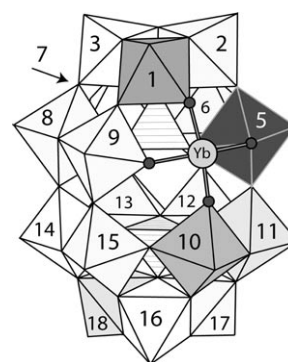


Figure 3. Numbering of  $[\alpha_1\text{-YbP}_2\text{W}_{17}\text{O}_{61}]^{7-}$  and graphical representation of the chemical-shift variation at different concentrations. The darkness of gray reflects the slope of the curves in Figure 2.

vironment between the monomer and the dimer, and dissociation of the dimer on dilution. Accordingly, the results suggest that dimerization occurs through W5-O-Yb' and W5'-O-Yb bridges. This arrangement also brings W1 and W10 into proximity of the second POM, as can be seen in the analogous dimeric  $\{\alpha_1\text{-Ce}\}_2$  in the solid state.<sup>[33]</sup> Thus, our methodology evidences dimerization in solution, and identifies which W=O group is involved. Dimerization in the solid state of the complex  $\{\alpha_1\text{-La}\}_2$  occurs through a capping W=O site.<sup>[44]</sup>

### Chiral differentiation

**Amino acids as ligands:** Pope et al. reported differentiation of the  $^{31}\text{P}$  NMR signals of  $\{\alpha_1\text{-Ce}\}$  by addition of enantiomerically pure amino acids, in particular L-proline.<sup>[33]</sup> We decided to follow this approach and recorded the spectra of a series of complexes  $\{\alpha_1\text{-Ln}\}$  ( $\text{Ln}=\text{La}^{\text{III}}, \text{Ce}^{\text{III}}, \text{Sm}^{\text{III}}, \text{Eu}^{\text{III}}$ ,

Nd<sup>III</sup>, Yb<sup>III</sup>) in the presence of increasing concentrations of L-proline. The results obtained in the presence of 20 equivalents of L-proline are summarized in Table 1. Each signal of { $\alpha_1$ -Ln} splits into two resonances, except for Ln=La, Sm, for which only the P1 signal splits. The amplitude of the splitting increases with increasing amount of ligand. This confirms the observations of Pope et al. and extends them to other { $\alpha_1$ -Ln} complexes.

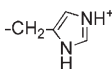
Table 1. Chiral differentiation by <sup>31</sup>P NMR of { $\alpha_1$ -Ln} in the presence of 20 equivalents of L-proline.

{ $\alpha_1$ -Ln}	$\Delta(\delta_{\text{obs}})$   (P1) [ppb]	$\Delta(\delta_{\text{obs}})$   (P2) [ppb]
La	30	0
Ce	160	70
Sm	60	0
Eu	60	30
Nd	130	40
Yb	250	300

The largest chiral differentiation is obtained for { $\alpha_1$ -Yb}, which may be attributable to larger paramagnetic shift of the complex.<sup>[42]</sup> Consequently, this complex was chosen for subsequent studies.

In the next step, <sup>31</sup>P NMR spectra of { $\alpha_1$ -Yb} in the presence of 20 equiv of a variety of amino acids were recorded (Table 2, Figure 4). It is not surprising, also by comparison with the reported results on { $\alpha_1$ -Ce},<sup>[33]</sup> that chiral differentiation depends on the nature of the amino acid. In the simplest way, chiral recognition can be explained by a three-point interaction between two chiral molecules. In the present case, the carboxylate group of the amino acid is expected to bind to the Yb ion, and the protonated  $\alpha$ -amino group should establish a hydrogen bond with a neighboring oxo ligand. The third interaction needed for chiral differentiation must involve the amino acid side chain. Evaluation of the splitting of <sup>31</sup>P NMR signals caused by different functional groups in the amino acid side chains allows some trends to be established, which have oriented our subsequent work. Chiral differentiation is rather weak with amino

Table 2. Chiral differentiation by <sup>31</sup>P NMR spectroscopy of { $\alpha_1$ -Yb} by a selection of amino acids (20 equiv). [{ $\alpha_1$ -Yb}] = 10 mmol L<sup>-1</sup>, T = 300 K.

Amino acid	Side chain	$\Delta(\delta_{\text{obs}})$   (P1) [ppb]	$\Delta(\delta_{\text{obs}})$   (P2) [ppb]
L-proline	alkylidene -(CH <sub>2</sub> ) <sub>5</sub> -	250	300
L-valine	alkyl -CH(CH <sub>3</sub> ) <sub>2</sub>	430	160
L-serine	alcohol -CH <sub>2</sub> OH	410	40
L-aspartate	acid -CH <sub>2</sub> COOH	50	0
L-glutamate	acid -(CH <sub>2</sub> ) <sub>2</sub> COOH	250	90
L-ornithine <sup>[a]</sup>	ammonium -(CH <sub>2</sub> ) <sub>3</sub> NH <sub>3</sub> <sup>+</sup>	350	320
L-lysine <sup>[a]</sup>	ammonium -(CH <sub>2</sub> ) <sub>4</sub> NH <sub>3</sub> <sup>+</sup>	310	310
L-arginine	guanidinium -(CH <sub>2</sub> ) <sub>3</sub> -NH-C(=NH <sub>2</sub> ) <sup>+</sup> NH <sub>2</sub>	1350	520
L-histidine	imidazolium -CH <sub>2</sub> - 	3400	440

[a] The hydrochloride of the amino acid was used.

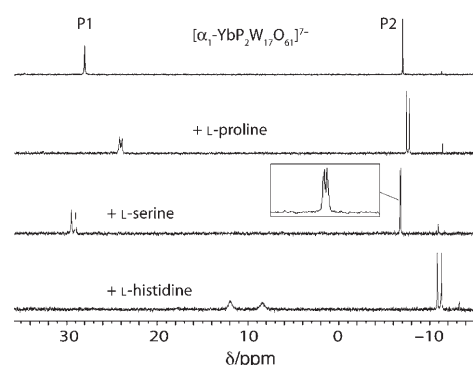


Figure 4. <sup>31</sup>P spectra of [ $\alpha_1$ -Yb(H<sub>2</sub>O)<sub>4</sub>P<sub>2</sub>W<sub>17</sub>O<sub>61</sub>]<sup>7-</sup> (10 mmol L<sup>-1</sup> in water, top) and in the presence of 20 equivalents of L-proline, L-serine, and L-histidine.

acids bearing carboxyl groups in their side chain, in particular with shorter chain length (aspartate versus glutamate). The most pronounced effects are obtained with L-arginine and L-histidine, two amino acids with protonated side chains under the experimental conditions. This may reflect the electrostatic attraction between the negatively charged POM and the positively charged side chain, which strengthens the interaction between { $\alpha_1$ -Yb} and the amino acid. Unfortunately, the <sup>31</sup>P and <sup>183</sup>W NMR signals are broadened to such an extent that a detailed analysis becomes impossible. In addition, the pH of these solutions is higher than for other amino acids, which compromises the long-term stability of the polyoxometalate. L-Lysine and L-ornithine, which also bear protonated side chains, exhibit smaller effects, likely because of the sterically less demanding functional group, which easily accommodates both enantiomers of { $\alpha_1$ -Yb}. The amino acids all produce comparable effects on P1 and P2, with two notable exceptions: L-serine and L-histidine, which influence P1 about ten times more than P2. The lack of flexibility of the side chains of serine and histidine may constrain these ligands in a particular orientation towards the YbPW<sub>8</sub> moiety of { $\alpha_1$ -Yb}, whereas for the other ligands a conformation implicating both sides of the POM

and/or a dynamic exchange between conformations would be possible. This particular behavior prompted us to investigate the system with L-serine more thoroughly, taking into account the drawbacks of L-histidine.

Assuming formation of a complex with 1:1 { $\alpha_1$ -Yb}:L-serine stoichiometry in a concentration range of 0.1 < [L-serine] < 0.6 mol L<sup>-1</sup> and 0.03 mol L<sup>-1</sup> { $\alpha_1$ -Yb}, the apparent formation constants were estimated from the variation in <sup>31</sup>P chemical shift of both P atoms. The obtained values of

$K_{11} = 1.7 \pm 1.0$  and  $K_{11} = 1.4 \pm 1.0$  for the two diastereomers have relatively large uncertainties, but they indicate the order of magnitude. They are slightly smaller than those found by Pope et al. for L-proline with  $\{\alpha_1\text{-Ce}\}$  and  $\{\alpha_2\text{-Ce}\}$ .<sup>[56]</sup>

$^{183}\text{W}$  NMR spectra in the presence of 10 and 20 equiv of L-serine were recorded at three different temperatures (Figure 5 and Supporting Information). The plots of the

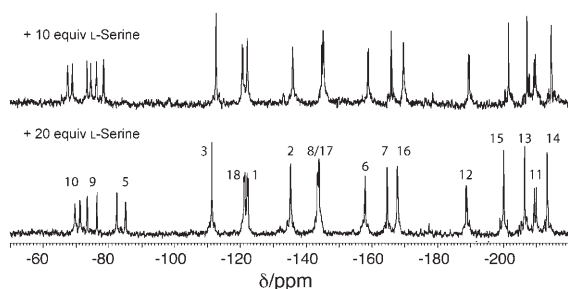


Figure 5.  $^{183}\text{W}$  NMR spectra of  $[\alpha_1\text{-Yb}(\text{H}_2\text{O})_4\text{P}_2\text{W}_{17}\text{O}_{61}]^{7-}$  in aqueous solution in the presence of L-serine with assignment of the peaks. Total concentration  $[\{\alpha_1\text{-Yb}\}] = 0.15 \text{ mol L}^{-1}$ .  $T = 293 \text{ K}$ .

temperature dependence of the chemical shifts allowed assignment of the peaks to the W atoms, by comparison with the chemical shifts and temperature coefficients obtained for  $\{\alpha_1\text{-Yb}\}$ . In some cases, the  $^2J_{\text{WW}}$  coupling constants were also measured to eliminate any ambiguity. The absence of a set of signals assignable to free  $\{\alpha_1\text{-Yb}\}$  indicates that both enantiomers of  $\{\alpha_1\text{-Yb}\}$  reacted with L-serine, as expected.

Figure 6 illustrates two effects of L-serine on each W site of  $\{\alpha_1\text{-Yb}\}$ . First, the ligand induces a variation in the chemical shifts of all signals, indicative of modification of the chemical environment of all W atoms. The largest changes are observed for W5, and to a smaller extent for W1 and W10, a result similar to the sensitivity of  $\delta_{\text{obs}}$  to POM concentration (see Figure 3). This is not surprising, because only the monomeric form of  $\{\alpha_1\text{-Yb}\}$  can react with L-serine, and therefore this complexation shifts the monomer–dimer equilibrium in the same manner as does dilution. Hence, variations in chemical shift are also expected for W atoms

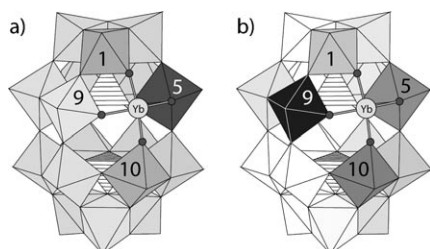


Figure 6. Influence of 10 equivalents of L-serine on the  $^{183}\text{W}$  NMR signals of  $[\alpha_1\text{-Yb}(\text{H}_2\text{O})_4\text{P}_2\text{W}_{17}\text{O}_{61}]^{7-}$ . a) The darkness of gray reflects the variation of chemical shifts  $\Delta_{\text{obs}}$  before and after addition of L-serine (see Figure 1). b) The darkness of gray reflects the difference between the chemical shifts of the diastereomers  $\Delta(\delta_{\text{obs}})$ .

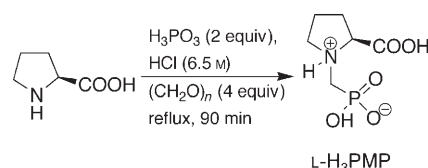
not directly involved in ligand binding but in dimerization. On the other hand, chemical-shift variations due to ligand complexation and dimer dissociation may compensate each other. As a result, the chemical shift variation does not allow the binding site of L-serine to be located.

The second effect of L-serine observed in the spectra of Figure 5 is that about half of the 17 signals are split. This indicates that these W sites are in different environments in the two diastereomers, and that the complex formed has the necessary rigidity to distinguish the influence of the ligand on the different W atoms. Figure 6b illustrates the amplitude of splitting at each site. This map directly reflects the interactions between the organic and inorganic molecules. The W atoms connected to  $\text{Yb}^{\text{III}}$  are more strongly influenced than those further away. This confirms the intuitive assumption that the serine ligand is bound to the Yb ion and to the neighboring oxygen atoms. It can then be assumed that the carboxylate group is coordinated to Yb, and that the ammonium group establishes a hydrogen bond to a nearby oxo ligand. Moreover, Figure 6b shows clearly that W9 is the most sensitive to the chirality of the ligand. This points to an orientation of the ligand in the belt of the Dawson structure. One possible arrangement in agreement with these observations would include a hydrogen bond between the  $\text{CH}_2\text{OH}$  side chain and an oxo ligand in the belt.

**Phosphonic acid derivatives as ligands:** We were not able to separate the two enantiomers of  $\{\alpha_1\text{-Yb}\}$  by crystallization of diastereomers formed with optically pure amino acids as ligand. Indeed, a large excess of ligand must be used to form a significant amount of complex, and under such conditions the amino acids crystallize first. This shifts the complexation equilibrium towards free  $\{\alpha_1\text{-Yb}\}$ . The problem might be overcome with a ligand with a stronger complexation constant. Furthermore, as noted above, the preparative separation of both diastereomers should be facilitated if they were present in different concentrations, and if their chemical properties were different. As we have shown for L-serine that this chiral recognition can be monitored by NMR spectroscopy, we sought a new ligand with a higher complexation constant and large chiral differentiation by this technique.

Among the known ligands for  $\text{Yb}^{3+}$  are phosphonate derivatives, and therefore we tried *N*-phosphonomethyl-L-proline (L- $\text{H}_3\text{PMP}$ , Scheme 1) because it combines several interacting groups.<sup>[58]</sup>

The two signals of  $\{\alpha_1\text{-Yb}\}$  in the  $^{31}\text{P}$  NMR spectrum split significantly in the presence of only one equivalent of L-



Scheme 1. Synthesis of *N*-phosphonomethyl-L-proline (L- $\text{H}_3\text{PMP}$ ).<sup>[58]</sup>



H<sub>3</sub>PMP, which indicates a higher complexation constant for phosphonate than for carboxylate, and good chiral recognition.

The method of continuous variations (Job plot) was used to determine the stoichiometry of the complex formed between { $\alpha_1$ -Yb} and L-H<sub>3</sub>PMP. The <sup>31</sup>P chemical shifts of P1, P2, and the P atom of the ligand were monitored while varying the molar fraction *X* of { $\alpha_1$ -Yb} and keeping a total concentration of 0.06 M (Figure 7). The Job plots for P1 and the

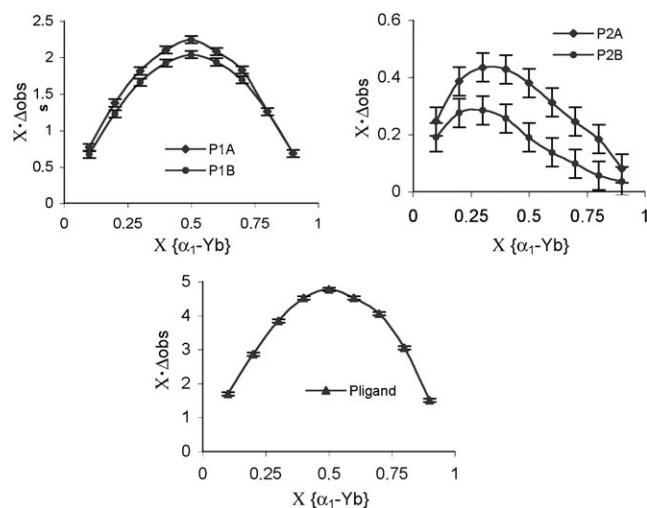


Figure 7. Job plots obtained by varying the molar fraction *X* of [ $\alpha_1$ -Yb-(H<sub>2</sub>O)<sub>4</sub>P<sub>2</sub>W<sub>17</sub>O<sub>61</sub>]<sup>7-</sup> with respect to L-H<sub>3</sub>PMP in aqueous solution (*c*<sub>total</sub> = 60 mmol L<sup>-1</sup>). Values measured by <sup>31</sup>P NMR spectroscopy for P1 and P2 in both diastereomers A and B, and for the P atom in the ligand.

ligand show a maximum at *X* = 0.5, which indicates a 1:1 stoichiometry of { $\alpha_1$ -Yb}:L-H<sub>3</sub>PMP. However, the maxima in the curves for P2 at *X* = 0.3 indicate 1:2 stoichiometry. This apparent contradiction must be explained by the presence of two complexes with similar formation constants. The method of continuous variations is limited in such a case. The chemical shifts of P1 and L-H<sub>3</sub>PMP must be very close, so that the 1:1 and 1:2 complexes cannot be distinguished. A similar situation is observed when using absorption spectroscopy to study equilibria of multiple complexes formed simultaneously in solution.<sup>[59]</sup> Job plots indicate different stoichiometries depending on the chosen wavelength in that case.

By use of the computer program HypNMR,<sup>[60]</sup> the stepwise complexation constants were determined from the chemical shifts observed at different concentrations. We found log(*K*<sub>11</sub>)<sub>A</sub> = 2.1 ± 0.4 and log(*K*<sub>12</sub>)<sub>A</sub> = 2.7 ± 0.4 for one diastereomer denoted A, and log(*K*<sub>11</sub>)<sub>B</sub> ≈ 2.6 and log(*K*<sub>12</sub>)<sub>B</sub> ≈ 3.3 for the other diastereomer denoted B. The *K* values are about two orders of magnitude larger than those obtained with natural amino acids.

As the stability of complexes with L-H<sub>3</sub>PMP is higher than that with amino acids, we analyzed the solution by ESI-MS.<sup>[44]</sup> The spectrum of K<sub>7</sub>{ $\alpha_1$ -Yb} recorded from a solution in H<sub>2</sub>O/CH<sub>3</sub>CN (1/1) shows a distribution of signals of

{ $\alpha_1$ -Yb} associated with K<sup>+</sup>, H<sup>+</sup>, and solvent molecules with overall charges of 5<sup>-</sup> and 4<sup>-</sup> for the molecular ion (Figure 8, top). After addition of 10 equivalents of L-

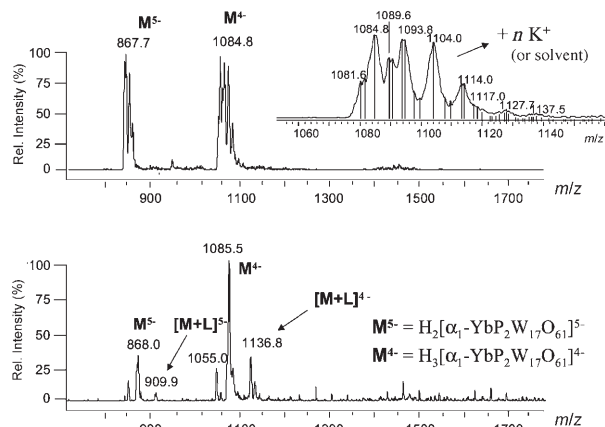


Figure 8. ESI mass spectra in H<sub>2</sub>O/CH<sub>3</sub>CN (1/1) solution. Top: { $\alpha_1$ -Yb-(H<sub>2</sub>O)<sub>4</sub>P<sub>2</sub>W<sub>17</sub>O<sub>61</sub>]<sup>7-</sup>, *c* = 50 μmol L<sup>-1</sup>. Bottom: after addition of 10 equivalents of L-H<sub>3</sub>PMP.

H<sub>3</sub>PMP, this distribution of adducts is no longer observed, and only the protonated species {H<sub>2</sub>[ $\alpha_1$ -YbP<sub>2</sub>W<sub>17</sub>O<sub>61</sub>]<sup>5-</sup> (*m/z* 868.0) and {H<sub>3</sub>[ $\alpha_1$ -YbP<sub>2</sub>W<sub>17</sub>O<sub>61</sub>]<sup>4-</sup> (*m/z* 1085.5) remain. Two new peaks arise at *m/z* 909.9 and 1136.8, corresponding to the addition of one ligand L-H<sub>3</sub>PMP to these anions. Thus, the ESI-MS analysis confirms the coordination of L-H<sub>3</sub>PMP to { $\alpha_1$ -Yb} by the signals for the 1:1 complex. The 1:2 complex cannot be seen under these conditions ([{ $\alpha_1$ -Yb}] = 50 μM, [L-H<sub>3</sub>PMP] = 500 μM), as its concentration is below nanomolar.

To gain further insight into the nature of the complex formed, <sup>183</sup>W NMR spectra were recorded in the presence of increasing amounts of L-H<sub>3</sub>PMP (Figure 9). Each solution was measured at different temperatures, and the temperature coefficients allowed some ambiguities in the assignment

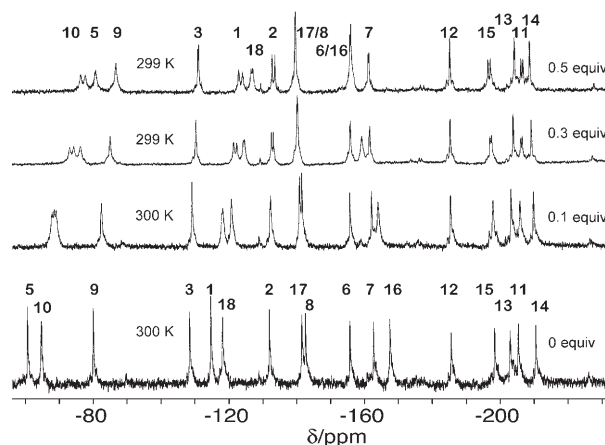


Figure 9. <sup>183</sup>W NMR spectra of [ $\alpha_1$ -Yb(H<sub>2</sub>O)<sub>4</sub>P<sub>2</sub>W<sub>17</sub>O<sub>61</sub>]<sup>7-</sup> (bottom) with increasing amounts of L-H<sub>3</sub>PMP in water. [ $\alpha_1$ -Yb(H<sub>2</sub>O)<sub>4</sub>P<sub>2</sub>W<sub>17</sub>O<sub>61</sub>]<sup>7-</sup> = 0.3 mol L<sup>-1</sup>, *T* = 299 or 300 K.

to be removed (see Supporting Information). Variation of the chemical shifts and splitting into two signals were observed for some of the peaks of  $\{\alpha_1\text{-Yb}\}$ , in line with the observations made with L-serine. As before, the signal of W5 is shifted the most, which reveals the change in the monomer-dimer equilibrium. Again, W atoms around the Yb ion are better differentiated by the chiral ligand, which confirms coordination to the Lewis acid site. However, there are pronounced differences between the effects of L-H<sub>3</sub>PMP and L-serine. The addition of as little as 0.1 equivalents of L-H<sub>3</sub>PMP allows chiral differentiation, whereas ten equivalents were necessary for amino acids. The W atoms that sense the chirality of the ligand are not the same as with L-serine, as can be seen by comparing Figure 6 with Figure 10.

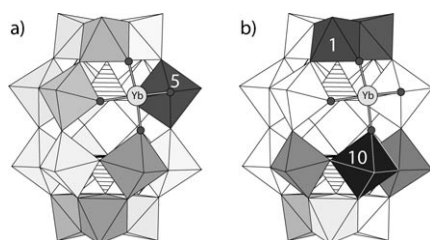


Figure 10. Influence of 0.5 equivalents of L-H<sub>3</sub>PMP on the <sup>183</sup>W signals of  $\{\alpha_1\text{-Yb}(\text{H}_2\text{O})_4\text{P}_2\text{W}_{17}\text{O}_{61}\}^{7-}$ . a) The darkness of gray reflects the variation of chemical shifts  $\Delta_{\text{obs}}$  before and after addition of L-H<sub>3</sub>PMP. b) The darkness of gray reflects the difference between the chemical shifts of the diastereomers  $\Delta(\delta_{\text{obs}})$ .

In the case of L-H<sub>3</sub>PMP, the largest  $|\Delta(\delta_{\text{obs}})|$  are found in two distinct areas around W1 and W10. W5 and W9 are not influenced, contrary to what was observed with L-serine. In accordance with the close stability of the two diastereomeric forms of  $\{\alpha_1\text{-Yb}\}\cdot\text{L-H}_3\text{PMP}$ , this observation may correspond to preferred interaction between the ligand and the cap of YbPW<sub>8</sub> for one of the  $\{\alpha_1\text{-Yb}\}$  enantiomers, and with the belt of the PW<sub>9</sub> moiety for the other enantiomer, that is, back-orientation of the ligand.

To evaluate the relative importance of the different functional groups on L-H<sub>3</sub>PMP, we also prepared its carboxymethyl ester. A small splitting of the <sup>31</sup>P NMR signals of  $\{\alpha_1\text{-Yb}\}$  is observed in the presence of this ligand. However, this compound is slowly hydrolyzed to L-H<sub>3</sub>PMP in solution, and the observed chiral differentiation may then result from the presence of L-H<sub>3</sub>PMP. Therefore, (R)-1-phosphonomethyl-2-methyl-pyrrolidine (R-H<sub>2</sub>PMMP) was prepared from (R)-(-)-2-methylpyrrolidine in 44% overall yield in a similar way as L-H<sub>3</sub>PMP (see Supporting Information).

Table 3 summarizes the interactions of proline and its derivatives with  $\{\alpha_1\text{-Yb}\}$ . We have to differentiate the primary interactions of the ligand with the Yb<sup>3+</sup> center, which determine the formation constant of the complex, from the secondary interactions involving peripheral O atoms of the POM, which are responsible for chiral differentiation.

The phosphonic acid is responsible for stronger complexation. It is known that phosphonate groups are better ligands

Table 3. Comparison of the complexation properties of  $\{\alpha_1\text{-Yb}\}$  with different ligands.

Ligand				
			L-H <sub>3</sub> PMP	R-H <sub>2</sub> PMMP
<i>K</i> (order of magnitude)	1	≤ 1	10 <sup>2</sup>	10 <sup>2</sup>
Differentiation of <sup>31</sup> P signals	+	-	++	-

for lanthanides than carboxylates, and carboxylic esters have no complexing properties at all. This allows the increased stability of the complexes of  $\{\alpha_1\text{-Yb}\}$  with L-H<sub>3</sub>PMP and R-H<sub>2</sub>PMMP compared to those with L-proline and its carboxymethyl ester to be understood. With the phosphonate as the primary anchoring group, the carboxylic acid appears to be a better auxiliary group for chiral recognition than a methyl group.

A working model for the arrangement of the ligand can be deduced from these results. The phosphonate group should be coordinated to the Yb ion, and the carboxyl group establishes a hydrogen bond with an oxo ligand. The ammonium group should also be in strong interaction with the polyoxometalate, by a combination of electrostatic attraction and hydrogen bonding. As a result, L-H<sub>3</sub>PMP has three important points of interaction with  $\{\alpha_1\text{-Yb}\}$  and leads to the observed chiral differentiation. The rigidity of the ligand is certainly a further advantage in this molecular-recognition process.

## Conclusion

Starting from the full assignment of the <sup>183</sup>W NMR spectra of  $\{\alpha_1\text{-Yb}\}$  at different concentrations, the most likely structure of the dimer in aqueous solution could be established.  $\{\alpha_1\text{-Yb}\}$  seems to dimerize through coordination of a belt W=O group to a neighboring complex. Such an arrangement is known for the complex  $\{\alpha_1\text{-Ce}\}$  in the solid state, and this analogy validates our approach.

Furthermore, screening of the effect of L-proline on the <sup>31</sup>P NMR spectra of a family of complexes  $\{\alpha_1\text{-Ln}\}$ , and of different amino acids on  $\{\alpha_1\text{-Yb}\}$ , allowed trends in the sensing of the chirality of  $\{\alpha_1\text{-Ln}\}$  by amino acids to be established. L-Serine was identified as a ligand with a particularly strong contrast in the differentiation of the P1 and P2 signals. The mapping of its influence on the W atoms confirmed experimentally the intuitive assumption of binding to the Yb ion. It also revealed that the chirality of the ligand is most strongly sensed by W9, a site in the YbPW<sub>8</sub> belt of the Dawson structure.

A phosphonic acid derivative of proline L-H<sub>3</sub>PMP was shown to exhibit much higher affinity than natural amino acids towards  $\{\alpha_1\text{-Yb}\}$ . Up to two such ligands bind to one

{ $\alpha_1$ -Yb} through coordination of the phosphonate group to the Yb ion. In this case, the chirality of the ligands influences the sites in the upper cap and the lower belt of the polyoxometalate.

More generally speaking, these results demonstrate how  $^{183}\text{W}$  NMR spectroscopy can be used to investigate the intermolecular interactions between an organic molecule and a polyoxometalate. In a nonsymmetric structure such as the  $\alpha_1$  monolacunary Dawson anion, all 17 W atoms can be monitored individually. The chemical shifts observed then reflect the chemical environments at each site. Yet, one should keep in mind that the surface of polyoxometalates is composed of closed-packed oxygen atoms. The observed chiral differentiation results from the chiral recognition of a metal oxide surface by an organic molecule. Such a molecular recognition process is of importance in the study of metal oxide catalysts for organic transformations. The { $\alpha_1$ -Yb} described herein can be used as a Lewis acid catalyst, and asymmetric catalysis should in principle be possible. We plan to model the exact arrangement of the ligands bound to { $\alpha_1$ -Yb} to gain further insight which will be useful for the design of resolving agents for { $\alpha_1$ -Yb} and the evaluation of potential substrates for asymmetric catalysis.

## Experimental Section

$\text{K}_7[\alpha_1\text{-Ln}(\text{H}_2\text{O})_n\text{P}_2\text{W}_{17}\text{O}_{61}]$  (Ln = La, Ce, Sm, Eu, Nd, Yb)<sup>[39,44]</sup> were prepared by literature methods, and checked by IR and  $^{31}\text{P}$  NMR spectroscopy.

$^{183}\text{W}$  NMR spectra were recorded in 10 mm o.d. tubes (sample volume 2.5 mL) at 12.5 MHz on a Bruker AC300 equipped with a low-frequency special VSP probe head, and at 20.8 MHz on a Bruker DRX500 spectrometer with a standard tunable BBO probe head. Chemical shifts are referenced to  $\text{WO}_4^{2-}$  ( $\delta = 0$  ppm) according to the IUPAC recommendation. Positive  $\delta$  corresponds to high-frequency shift (deshielding) with respect to the reference. They were measured by the substitution method, by using a saturated solution of dodecatungstosilicic acid ( $\text{H}_4\text{SiW}_{12}\text{O}_{40}$ ) in  $\text{D}_2\text{O}$  as secondary standard ( $\delta = -103.8$  ppm). The spectral width was about 200 ppm. At 12.5 MHz, high-quality spectra with signal-to-noise ratio good enough to observe tungsten satellites required at least  $10^5$  transients corresponding to more than 2 days of spectrometer time; 12 h of acquisition time was sufficient to observe the signals for all 17 W atoms. Concentrated solutions were obtained by cation exchange with  $\text{LiClO}_4$ .

$^{31}\text{P}$  spectra were recorded in 5 mm o.d. tubes at 121.5 MHz on a Bruker AC300/Avance II 300 equipped with a QNP probe head. Chemical shifts are referenced to 85%  $\text{H}_3\text{PO}_4$ .  $^{31}\text{P}$  spectra were also measured prior to  $^{183}\text{W}$  spectra on the same NMR tubes on the decoupling coil of the VSP probe head, both for control and for determination of the  $^{31}\text{P}$  decoupling frequency. The  $^{31}\text{P}$  decoupling experiments were performed with a B-SV3 unit operating at 121.5 MHz and equipped with a B-BM1 broadband modulator. Selective or broadband decoupling was determined by appropriate choice of the synthesizer frequency and of the output power (5–40 W) before entering the decoupling coil of the low-frequency probe head.

The following conditions were used for binding studies by  $^{183}\text{W}$  NMR spectroscopy: with L-serine: [ $\{\alpha_1\text{-Yb}\}$ ] =  $0.14 \text{ mol L}^{-1}$ ,  $T = 288\text{--}303 \text{ K}$ ; with L- $\text{H}_3\text{PMP}$ : [ $\{\alpha_1\text{-Yb}\}$ ] =  $0.33 \text{ mol L}^{-1}$ ,  $T = 280\text{--}320 \text{ K}$ . Ligands were added as solids. Further details are available in the Supporting Information.

## Acknowledgements

This work was supported by University Pierre and Marie Curie, CNRS, and IUF, of whom M.M. is a senior member, and ANR (grant JC05\_41806 to E.L., S.T., and B.H.). C.B. thanks the Ministère de la recherche and IUF and P.R. thanks ANR for fellowships. We thank Prof. Jean-Claude Tabet, and Dr. Carlos Afonso (UPMC) for the MS analysis. Prof. Didier Villemin (Caen) is gratefully acknowledged for a generous gift of L- $\text{H}_3\text{PMP}$  that allowed initial studies.

- [1] D. L. Long, E. Burkholder, L. Cronin, *Chem. Soc. Rev.* **2007**, *36*, 105–121.
- [2] *Polyoxometalate Molecular Science*. (Eds. J. J. Borrás-Almenar, E. Coronado, A. Müller, M. T. Pope), *NATO Sci. Ser. II, Vol. 98*, Kluwer, Dordrecht, **2003**.
- [3] M. T. Pope, A. Müller, *Top. Mol. Org. Eng.* **1994**, *12*, 411.
- [4] X. Fang, T. M. Anderson, Y. Hou, C. L. Hill, *Chem. Commun.* **2005**, 5044–5046.
- [5] U. Kortz, M. G. Savelieff, F. Y. A. Ghali, L. M. Khalil, S. A. Maalouf, D. I. Sinno, *Angew. Chem.* **2002**, *114*, 4246–4249; *Angew. Chem. Int. Ed.* **2002**, *41*, 4070–4073.
- [6] M. Lu, J. Kang, D. Wang, Z. Peng, *Inorg. Chem.* **2005**, *44*, 7711–7713 (Erratum p. 9977).
- [7] M. Inoue, T. Yamase, *Bull. Chem. Soc. Jpn.* **1996**, *69*, 2863–2868.
- [8] M. Inoue, T. Yamase, *Bull. Chem. Soc. Jpn.* **1995**, *68*, 3055–3063.
- [9] S. Bareyt, S. Piligkos, B. Hasenknopf, P. Gouzerh, E. Lacôte, S. Thorimbert, M. Malacria, *J. Am. Chem. Soc.* **2005**, *127*, 6788–6794.
- [10] K. Micoine, B. Hasenknopf, S. Thorimbert, E. Lacôte, M. Malacria, *Org. Lett.* **2007**, *9*, 3981–2984.
- [11] C. Streb, L. Long, L. Cronin, *Chem. Commun.* **2007**, 471–473.
- [12] H.-Y. An, E.-B. Wang, D.-R. Xiao, Y.-G. Li, Z.-M. Su, L. Xu, *Angew. Chem.* **2006**, *118*, 918–922; *Angew. Chem. Int. Ed.* **2006**, *45*, 904–908.
- [13] R. Y. Wang, D. Z. Jia, L. Zhang, L. Liu, Z. P. Guo, B. Q. Li, J. X. Wang, *Adv. Funct. Mater.* **2006**, *16*, 687–692.
- [14] X. Fang, T. M. Anderson, C. L. Hill, *Angew. Chem.* **2005**, *117*, 3606–3610; *Angew. Chem. Int. Ed.* **2005**, *44*, 3540–3544.
- [15] B. S. Bassil, M. H. Dickman, U. Kortz, *Inorg. Chem.* **2006**, *45*, 2394–2396.
- [16] F. Xin, M. T. Pope, *J. Am. Chem. Soc.* **1996**, *118*, 7731–7736.
- [17] C. M. Tourné, G. F. Tourné, F. Zonnevillie, *J. Chem. Soc. Dalton Trans.* **1991**, 143–155.
- [18] R. Acerete, J. Server-Carrió, A. Vegas, M. Martínez-Ripoll, *J. Am. Chem. Soc.* **1990**, *112*, 9386–9387.
- [19] M. H. Alizadeh, S. P. Harmalker, Y. Jeannin, J. Martin-Frère, M. T. Pope, *J. Am. Chem. Soc.* **1985**, *107*, 2662–2669.
- [20] M. T. Pope, *Inorg. Chem.* **1976**, *15*, 2008–2010.
- [21] T. Ama, J. Hidaka, Y. Shimura, *Bull. Chem. Soc. Jpn.* **1970**, *43*, 2654.
- [22] T. Yasui, T. Ama, G. B. Kauffman, *J. Chem. Educ.* **1989**, *66*, 1045–1048.
- [23] E. Coronado, S. Curreli, C. Giménez-Saiz, C. J. Gómez-García, J. Roth, *Synth. Met.* **2005**, *154*, 241–244.
- [24] U. Kortz, S. Matta, *Inorg. Chem.* **2001**, *40*, 815–817.
- [25] H. Tan, Y. Li, Z. Zhang, C. Qin, X. Wang, E. Wang, Z. Su, *J. Am. Chem. Soc.* **2007**, *129*, 10066–10067.
- [26] Y. Hou, X. Fang, C. L. Hill, Abstracts of Papers, 232nd ACS National Meeting, San Francisco, CA, USA, Sept. 10–14, **2006**, INOR-815.
- [27] The Pfeiffer effect is the change in optical rotation, and the induced Cotton effect the change in the circular dichroism spectrum, of an optically active substance on addition of a racemic mixture of a chiral, optically labile compound.
- [28] J. F. Garvey, M. T. Pope, *Inorg. Chem.* **1978**, *17*, 1115–1118.
- [29] V. Shivaiah, T. Arumuganathan, S. K. Das, *Inorg. Chem. Commun.* **2004**, *7*, 367–369.
- [30] K. Nomiya, R. Kobayashi, M. Miwa, *Bull. Chem. Soc. Jpn.* **1983**, *56*, 3505–3506.
- [31] K. Nomiya, R. Kobayashi, M. Miwa, T. Hori, *Polyhedron* **1984**, *3*, 1071–1076.



- [32] K. Nomiya, M. Miwa, Y. Sugaya, *Polyhedron* **1984**, *3*, 381–383.
- [33] M. Sadakane, M. H. Dickman, M. T. Pope, *Inorg. Chem.* **2001**, *40*, 2715–2719.
- [34] C. Boglio, G. Lemiere, B. Hasenknopf, S. Thorimbert, E. Lacôte, M. Malacria, *Angew. Chem.* **2006**, *118*, 3402–3405; *Angew. Chem. Int. Ed.* **2006**, *45*, 3324–3327.
- [35] C. Boglio, K. Micoine, P. Rémy, B. Hasenknopf, S. Thorimbert, E. Lacôte, M. Malacria, C. Afonso, J.-C. Tabet, *Chem. Eur. J.* **2007**, *13*, 5426–5432.
- [36] R. D. Peacock, T. J. R. Weakley, *J. Chem. Soc. A* **1971**, 1836–1839.
- [37] J.-P. Ciabrini, R. Contant, *J. Chem. Res. Miniprint* **1993**, 2720–2744.
- [38] J. Bartis, M. Dankova, M. Blumenstein, L. C. Francesconi, *J. Alloys Compd.* **1997**, *249*, 56–68.
- [39] J. Bartis, M. Dankova, J. J. Lessmann, Q.-H. Luo, W. D. Horrocks, Jr., L. C. Francesconi, *Inorg. Chem.* **1999**, *38*, 1042–1053.
- [40] Q.-H. Luo, R. C. Howell, M. Dankova, J. Bartis, C. W. Williams, W. D. Horrocks, Jr., V. G. Young, A. L. Rheingold, L. C. Francesconi, M. R. Antonio, *Inorg. Chem.* **2001**, *40*, 1894–1901.
- [41] C. Zhang, R. C. Howell, K. B. Scotland, F. G. Perez, L. Todaro, L. C. Francesconi, *Inorg. Chem.* **2004**, *43*, 7691–7701.
- [42] C. Zhang, R. C. Howell, Q.-H. Luo, H. L. Fieselmann, L. J. Todaro, L. C. Francesconi, *Inorg. Chem.* **2005**, *44*, 3569–3578.
- [43] Q. Lunyu, W. Shouguo, P. Jun, C. Yaguang, *Polyhedron* **1992**, *11*, 2645–2649.
- [44] C. Boglio, G. Lenoble, C. Duhayon, B. Hasenknopf, R. Thouvenot, C. Zhang, R. C. Howell, B. P. Burton-Pye, L. C. Francesconi, E. Lacôte, S. Thorimbert, M. Malacria, C. Afonso, J.-C. Tabet, *Inorg. Chem.* **2006**, *45*, 1389–1398.
- [45] C. Zhang, L. Bensaid, D. McGregor, X. F. Fang, R. C. Howell, B. Burton-Pye, Q.-H. Luo, L. Todaro, L. C. Francesconi, *J. Cluster Sci.* **2006**, *17*, 389–425.
- [46] Y. Lu, Y. Xu, Y. Li, E. Wang, X. Xu, Y. Ma, *Inorg. Chem.* **2006**, *45*, 2055–2060.
- [47] P. Mialane, A. Dolbecq, J. Marrot, F. Sécheresse, *Inorg. Chem. Commun.* **2005**, *8*, 740–742.
- [48] N. Belai, M. H. Dickman, M. T. Pope, R. Contant, B. Keita, I. M. Mbomekalle, L. Nadio, *Inorg. Chem.* **2005**, *44*, 169–171.
- [49] J. Y. Niu, J. W. Zhao, D. J. Guo, J. P. Wang, *J. Mol. Struct.* **2004**, *692*, 223–229.
- [50] U. Kortz, *J. Cluster Sci.* **2003**, *14*, 205–214.
- [51] Q.-H. Luo, R. C. Howell, J. Bartis, M. Dankova, W. D. Horrocks, Jr., A. L. Rheingold, L. C. Francesconi, *Inorg. Chem.* **2002**, *41*, 6112–6117.
- [52] J. Bartis, S. Sukal, M. Dankova, E. Kraft, R. Kronzon, M. Blumenstein, L. C. Francesconi, *J. Chem. Soc. Dalton Trans.* **1997**, 1937–1944.
- [53] A. Ostuni, R. E. Bachman, M. T. Pope, *J. Cluster Sci.* **2003**, *14*, 431–446.
- [54] B. S. Bassil, M. H. Dickman, B. Von Kammer, U. Kortz, *Inorg. Chem.* **2007**, *46*, 2452–2458.
- [55] C. Zhang, R. C. Howell, D. McGregor, L. Bensaid, S. Rahyab, M. Nayshtut, S. Lekperic, L. C. Francesconi, *C. R. Chimie* **2005**, *8*, 1035–1044.
- [56] M. Sadakane, A. Ostuni, M. T. Pope, *J. Chem. Soc. Dalton Trans.* **2002**, 63–67.
- [57] G. Lenoble, B. Hasenknopf, R. Thouvenot, *J. Am. Chem. Soc.* **2006**, *128*, 5735–5744.
- [58] A. Turner, P.-A. Jaffres, E. J. MacLean, D. Villemain, V. McKee, G. B. Hix, *Dalton Trans.* **2003**, 1314–1319.
- [59] W. C. Vosburgh, G. R. Cooper, *J. Am. Chem. Soc.* **1941**, *63*, 437–442.
- [60] C. Frassinetti, S. Ghelli, P. Gans, A. Sabatini, M. S. Moruzzi, A. Vacca, *Anal. Biochem.* **1995**, *231*, 374–382.

Received: September 11, 2007  
Published online: November 23, 2007